Kalman-Like Filter Under Binary Sensors

Zhongyao Hu, Bo Chen, *Member, IEEE*, Yuchen Zhang, *Graduate Student Member, IEEE*, and Li Yu, *Member, IEEE*

***Abstract*— This article is concerned with the Kalman-like filtering (KLF) problem for linear and nonlinear dynamic systems observed by binary sensors. Binary sensors are a special class of sensors that output only one bit of data and have considerable advantages in terms of energy consumption and economic costs. However, it is difficult to directly use binary sensors to estimate system states since the available information is compressed to the extreme and is difficult to be extracted. To address this problem, this article proposes an uncertainty measurement model to capture the innovations generated from binary sensors by analyzing their characteristics. Based on the proposed model, the KLFs are constructed for linear and nonlinear dynamical systems. Then, to deal with the uncertainties induced by binary sensors, conservative error covariances with adjustable parameters are derived for the KLFs via matrix inequalities and unscented transform. The optimal filter gains and some adjustable parameters are obtained by minimizing the traces and the upper bounds of the conservative covariances, respectively. Finally, arterial O_2 system and damped mass-spring system are employed to show the effectiveness and advantages of the proposed methods.**

***Index Terms*— Binary sensor, Kalman-like filter (KLF), state estimation, unscented transform.**

I. Introduction

KALMAN filter [1] is the minimum mean square error estimator for linear Gaussian systems, which have the advantages of high accuracy, low computational effort, and ease of implementation. In fact, a large number of practical systems are nonlinear, which limits the application of the Kalman filter. In this case, a series of Kalman-like filters (KLFs) such as extended Kalman filter [2], unscented Kalman filter [3], and cubature Kalman filter [4] have been proposed, and these nonlinear filters share a similar structure as the Kalman filter. Notice that the above methods are developed based on traditional continuous-value sensors which transmit sensor data completely. However, sensor energy and bandwidth constraints in the communication environment are frequent problems, and thus under these situations, sensor data cannot be transmitted completely. To overcome the above-mentioned problems, different KLFs have been proposed based on the quantization method [5]-[8] and the dimensionality reduction method [9]–[11], and these methods can reduce the size of the sensor data being transmitted.

Binary sensors are a special type of sensors that output only one bit of data. Obviously, binary sensors can minimize the size of the data being transmitted, and thus the problems of energy and bandwidth limitations are naturally avoided. Particularly, binary sensors are cost-effective, which makes them very flexible in the application, that is, different performance requirements can be met by arranging different numbers of binary sensors. Attracted by these advantages, research on target tracking [12]-[16] and non-cooperative target detection [17]-[19] by means of binary sensors has been carried out long ago. In these two problems, the sensor transmits "1" only when it measures that the distance between itself and the target is less than a threshold set in advance. Moreover, the inexpensive heated exhaust gas oxygen sensor [20], which switches its outputs when the air-to-fuel ratio in the exhaust gas crosses the stoichiometric value, is a typical binary sensor and is often utilized in automotive emission control to save economic costs. Furthermore, in the field of system identification, binary sensors have been utilized to solve parameter estimation problem under low power requirements [21]. More recently, there has been a growing interest in binary sensors in popular fields, such as medicine [22] and cyber physical systems [23]. The above facts illustrate that binary sensors have broad application prospects in the practical engineering.

However, state estimation using binary sensors is a very tricky business because only one bit of information is available. To deal with the high nonlinearity of the binary output (similar to the step signal), most of the existing filtering algorithms based on binary sensors were designed by using the Monte Carlo (MC) method, such as the target tracking algorithms in [14] and [15]. However, the MC method is computationally burdensome and contradicts the original intention of lightweight design of the binary sensors system. The work in [24] and [25] adopted an information feedback approach to change the threshold of the binary sensor, which does enable more information being contained in the one bit output. In fact, receiving a complete data (e.g., 64 bits) requires more energy, which is contrary to the advantage of binary sensors in low energy consumption. On the other hand, a class of threshold-based methods for processing binary outputs has also received a great deal of attention. This method can extract useful information from binary sensors by analyzing their intrinsic measurement form and then avoid dealing with the high nonlinearity of the binary outputs directly. In [26]–[28], the thresholds of binary sensors were modeled as convex

Manuscript received December 18, 2021; accepted January 23, 2022. Date of publication February 7, 2022; date of current version March 4, 2022. This work was supported in part by the Natural Science Foundation of China under Grant 61973277 and Grant 62073292 and in part by the Zhejiang Provincial Natural Science Foundation of China under Grant LR20F030004. The Associate Editor coordinating the review process was Dr. Susanna Spinsante. *(Corresponding author: Bo Chen.)*

The authors are with the Department of Automation and the Institute of Cyberspace Security, Zhejiang University of Technology, Hangzhou 310023, China (e-mail: huzhongyao@aliyun.com; bchen@aliyun.com; yuchenzhang95@163.com; lyu@zjut.edu.cn).

Digital Object Identifier 10.1109/TIM.2022.3149327

TABLE I
MAIN DISTINCTIVE CHARACTERISTICS OF THE MENTIONED BINARY SENSOR-RELATED WORK

References	Problem of interest	Information extraction	Threshold	Consumption	Methods
[14]-[15]	Target tracking	Sensor coordinate & threshold	Fixed	Low	MC
[12]					Euclid geometry
[16]					Maximum likelihood
[17]-[19]	Non-cooperative target detection	Local decision	Fixed	Low	Hypothesis testing
[21]	System identification	Threshold	Fixed	Low	Min-Max optimization
[24]	State estimation	Quantified innovation	Time-varying	Moderate	Bayesian filter
[25]					MC
[26]		Switching information	Fixed	Low	MHE
[27]					Distributed fusion Kalman
[28]					Bounded recursion
This paper		Innovation			Kalman-like filter

combinations of two sensed variables with uncertainties, and then, moving horizon estimation (MHE) and distributed fusion KLF (DFKLF) for binary sensors were proposed in [26] and [27] based on the threshold model. Subsequently, by using the bounded recursion method [29], [28] extended DFKLF to the case where the statistical properties of the system noise were unknown, but it is computationally intensive as the optimization algorithm is needed to solve the linear matrix inequality. It should be pointed that the above threshold-based methods all have two common shortcomings: 1) the uncertainties in the model are ignored when designing filters, which would reduce their estimation performance and 2) these methods are only applicable to the linear dynamic systems, but many practical systems are nonlinear.

Motivated by the above analysis, we shall study the KLF problem for linear/nonlinear dynamic systems observed by binary sensors. The main contributions of this article are summarized as follows.

1) A novel innovation-based uncertainty model for binary sensor is developed, which can extract more useful information for KLFs than the switch-based uncertainty model in [26]–[28]. Meanwhile, when the novel model is employed to construct KLFs, the uncertainties induced by binary sensors can be offset rather than ignored directly as in [26]–[28].
2) Based on the proposed new model, KLFs are designed for both linear and nonlinear dynamic systems under binary sensors, and the filter gains are obtained by minimizing the traces of estimation error covariances. Meanwhile, by minimizing the upper bound of the estimation error covariances, an optimal selection criterion for some adjustable parameters in the KLFs is developed to reduce the unreliability caused by experience. Furthermore, since only a small part of the binary measurements need to be augmented, the computational burden of the proposed KLFs are much lower than that of the traditional centralized algorithms.

Table I categorizes the reviewed works along their main distinctive characteristics so as to better position the study of this article. An outline of this article is as follows: Section II formulates the problem of interest and develops a new innovation-based uncertainty model for binary sensors. In Section III, linear and nonlinear KLFs are constructed using the new model, and the corresponding optimal filter gains are derived. Several simulations are presented in Section IV

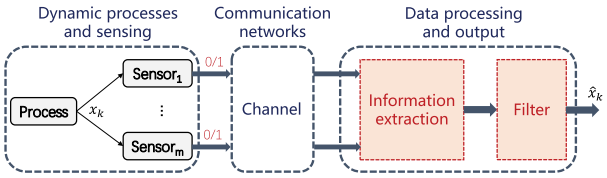

Fig. 1. Block diagram of the state estimation system with binary measurements. The work of this article is developed for information extraction and filter design, that is, the red part of this figure.

to verify the effectiveness and advantages of the proposed methods. Section V concludes the full article and provides an outlook on future work.

Notations: $\mathbb{R}^r$ and $\mathbb{R}^{r\times s}$ denote the r-dimensional and $r\times s$-dimensional Euclidean spaces, respectively. $E\{\cdot\}$ denotes mathematical expectation, while diag$\{\cdot\}$ stands for block diagonal matrix. O is the zero matrix and I stands for the identity matrix. Tr$(\cdot)$ represents the trace of the matrix. For a matrix $A\in\mathbb{R}^{r\times r}$, its eigenvalues are denoted by $\lambda_i(A)$, $i=1,2,\ldots,r$, where the largest eigenvalue is denoted as $\lambda_{\max}(A)$. $d_i(A)$ stands for the ith diagonal element of A and $d_{\max}(A)$ represents the largest diagonal element. For a matrix B, B_i denotes the ith column of B. For $X\in\mathbb{R}^{r\times r}$, $Y\in\mathbb{R}^{r\times r}$, $X>Y$, and $X\geq Y$, respectively, mean that X–Y is a positive definite matrix and a semi-positive definite matrix.

II. PROBLEM FORMULATION

Consider the dynamic system shown in Fig. 1, whose state-space model can be expressed as

$$\begin{cases} x_k = f(x_{k-1},u_{k-1})+C_{k-1}w_{k-1} \\ y_k^i = \begin{cases} 1, & z_k^i\geq\tau^i \\ 0, & z_k^i<\tau^i, \end{cases} \quad i=1,2,\ldots,m \end{cases} \tag{1}$$

where the sensed variable z_k^i of the binary sensor i is given by

$$z_k^i = h^i(x_k)+E_k^i v_k^i.$$

Here, $x_k\in\mathbb{R}^n$ is the system state and $y_k^i\in\mathbb{R}^1$ is the ith binary measurement. τ^i is the threshold of the ith binary sensor, which is a constant. u_{k-1} is the control input. $f(\cdot)\in\mathbb{R}^n$ and $h(\cdot)\in\mathbb{R}^1$ are arbitrary nonlinear functions, C_{k-1} and E_k^i are matrices with appropriate dimensions. w_k, v_k^i, and v_k^j, $i\neq j$, are uncorrected Gaussian white noises, and their covariances are Q_k, R_k^i, and R_k^j, respectively. Moreover, when

the system state x_k and the sensed variable z_k^i are both linear, the system (1) reduces to

$$\begin{cases} x_k = A_{k-1}x_{k-1} + B_{k-1}u_{k-1} + C_{k-1}w_{k-1} \\ y_k^i = \begin{cases} 1, & z_k^i \geq \tau^i \\ 0, & z_k^i < \tau^i, \end{cases} \quad i = 1, 2, \ldots, m \end{cases} \tag{2}$$

where

$$z_k^i = D_k^i x_k + E_k^i v_k^i.$$

Here, A_{k-1}, B_{k-1}, and D_k^i are matrices with appropriate dimensions.

As can be seen from the definition of y_k^i in (1) and (2), binary sensors hardly provide valid information from outputs of one bit. Therefore, a novel uncertain measurement model will be developed to extract useful information from binary sensors. To this end, let us define

$$\bar{y}_k^i \triangleq \begin{cases} 1, & \bar{z}_k^i \geq \tau^i \\ 0, & \bar{z}_k^i < \tau^i, \end{cases} \quad i = 1, 2, \ldots, m \tag{3}$$

where $\bar{z}_k^i$ is the one-step prediction of the sensed variable z_k^i. By comparing the definitions of y_k^i and $\bar{y}_k^i$, we know that, when $y_k^i \neq \bar{y}_k^i$, threshold τ^i will inevitably fall between $\bar{z}_k^i$ and z_k^i, which can be modeled as

$$\tau^i = \left(0.5 - \delta_k^i\right)\bar{z}_k^i + \left(0.5 + \delta_k^i\right)z_k^i, \quad i \in \mathcal{I}_k \tag{4}$$

where $\delta_k^i \in (-0.5, 0.5)$ is an uncertain parameter whose exact value is unknown. $\mathcal{I}_k$ represents the index set of the binary sensors whose output $y_k^i \neq \bar{y}_k^i$, which can be denoted as

$$\mathcal{I}_k = \left\{i \middle| \bar{y}_k^i \neq y_k^i\right\}. \tag{5}$$

Notice that the model (4) represents the threshold as a convex combination of $\bar{z}_k^i$ and z_k^i, and thus it can effectively extract the intrinsic measurement information of binary sensors.

Consequently, the purpose of this article is to design KLFs for systems (1) and (2) based on the model (4) such that the mean-square errors of KLFs are minimal at each time.

Remark 1: It is well known that the KLFs correct the one-step prediction after receiving the measurements from sensors, and thus obtain state estimate. In fact, the correction is needed because measurements contain new information that differs from the one-step prediction. This new information is the part of the measurement that really plays a role in the filter and is often referred to as innovation. According to (1) and (2), we know that the information contained in the binary measurement $y_k^i = 1$ is $z_k^i \geq \tau^i$. Then, if the one-step prediction $\bar{z}_k^i \geq \tau^i$ (i.e., $\bar{y}_k^i = 1$), the information contained in the binary measurement will overlap with that of the one-step prediction. In this case, only little innovation is contained in y_k^i. Moreover, the same conclusion can be obtained at $y_k^i = \bar{y}_k^i = 0$. Therefore, when the binary measurements do not belong to $\mathcal{I}_k$, they have little effect on the filter. On the contrary, the binary measurements belonging to $\mathcal{I}_k$, which contain more innovations, play a major role in the filter. Based on this idea, it is proposed to extract the useful information from the binary measurements that belong to $\mathcal{I}_k$ and then the innovation-based model (4) is developed in this article.

Remark 2: When y_k^i changes (i.e., $y_k^i \neq y_{k-1}^i$), one can deduce that the threshold τ^i must fall into the interval between z_{k-1}^i and z_k^i. To describe this phenomenon, a swith-based model was proposed in [26]–[28] as follows:

$$\tau^i = \left(0.5 - \epsilon_k^i\right)z_{k-1}^i + \left(0.5 + \epsilon_k^i\right)z_k^i, \quad i \in \mathcal{S}_k \tag{6}$$

where $\epsilon_k^i \in (-0.5, 0.5)$ was an uncertain parameter and $\mathcal{S}_k = \{i | y_{k-1}^i \neq y_k^i\}$. Though model (6) is reasonable, it only captures the switching information in the binary measurements instead of the innovation. In fact, it has been pointed out that the innovation of the measurement plays a major role in the KLFs. Under this case, model (4) is considered to capture more information that is useful for the KLF than model (6).

III. Designing KLFs

Before giving the main results of this article, the number of sensors belonging to $\mathcal{I}_k$ is first defined as m_k, and

$$\begin{cases} z_{\mathcal{I},k} \triangleq [z_k^{i_{k1}} \ \cdots \ z_k^{i_{km_k}}]^T \ \bar{z}_{\mathcal{I},k} \triangleq [\bar{z}_k^{i_{k1}} \ \cdots \ \bar{z}_k^{i_{km_k}}]^T \\ \tau_{\mathcal{I},k} \triangleq [\tau^{i_{k1}} \ \cdots \ \tau^{i_{km_k}}]^T \ v_{\mathcal{I},k} \triangleq [v_k^{i_{k1}} \ \cdots \ v_k^{i_{km_k}}]^T \\ D_{\mathcal{I},k} \triangleq [(D_k^{i_{k1}})^T \ \cdots \ (D_k^{i_{km_k}})^T]^T \\ E_{\mathcal{I},k} \triangleq \operatorname{diag}(E_k^{i_{k1}}, \ldots, E_k^{i_{km_k}}), \quad i_{k1}, \ldots, i_{km_k} \in \mathcal{I}_k \\ h_{\mathcal{I},k}(\cdot) \triangleq [h^{i_{k1}}(\cdot) \ \cdots \ h^{i_{km_k}}(\cdot)]^T \\ R_{\mathcal{I},k} \triangleq \operatorname{diag}(R_k^{i_{k1}}, \ldots, R_k^{i_{km_k}}) \\ \Delta_{\mathcal{I},k} \triangleq \operatorname{diag}(\delta_k^{i_{k1}}, \ldots, \delta_k^{i_{km_k}}). \end{cases} \tag{7}$$

A. KLF for Linear Systems With Binary Sensors

In this section, the KLF problem for system (2) will be solved. To this end, $\mathcal{I}_k$ needs to be determined first. For system (2), the one-step prediction $\bar{z}_k^i$ of the sensed variable z_k^i can be calculated as

$$\bar{z}_k^i = D_k^i \bar{x}_k, \quad i = 1, 2, \ldots, m \tag{8}$$

where the one-step state prediction $\bar{x}_k$ is given by

$$\bar{x}_k = A_{k-1}\hat{x}_{k-1} + B_{k-1}u_{k-1}. \tag{9}$$

Then, $\mathcal{I}_k$ can be easily determined by (3), (5), and (8). Augmenting these binary measurements that belong to $\mathcal{I}_k$, one has

$$z_{\mathcal{I},k} = D_{\mathcal{I},k}x_k + E_{\mathcal{I},k}v_{\mathcal{I},k} \tag{10}$$

$$\bar{z}_{\mathcal{I},k} = D_{\mathcal{I},k}\bar{x}_k \tag{11}$$

$$\tau_{\mathcal{I},k} = \left(0.5I - \Delta_{\mathcal{I},k}\right)\bar{z}_{\mathcal{I},k} + \left(0.5I + \Delta_{\mathcal{I},k}\right)z_{\mathcal{I},k} \tag{12}$$

where $z_{\mathcal{I},k}$, $\bar{z}_{\mathcal{I},k}$, $v_{\mathcal{I},k}$, $E_{\mathcal{I},k}$, $D_{\mathcal{I},k}$, $\Delta_{\mathcal{I},k}$, and $\tau_{\mathcal{I},k}$ are defined in (7). As can be seen from (12) that the threshold $\tau_{\mathcal{I},k}$ is represented as a linear transformation of $z_{\mathcal{I},k}$, and hence the one-step prediction of (12) can be given by

$$\bar{\tau}_{\mathcal{I},k} = \left(0.5I - \Delta_{\mathcal{I},k}\right)\bar{z}_{\mathcal{I},k} + \left(0.5I + \Delta_{\mathcal{I},k}\right)\bar{z}_{\mathcal{I},k} = \bar{z}_{\mathcal{I},k}. \tag{13}$$

Treating (12) as the measurement equation, the state estimate $\hat{x}_k$ for system (2) can be constructed as the KLF structure

$$\begin{cases} \hat{x}_k = \bar{x}_k + G_{\mathcal{I},k}^L\left(\tau_{\mathcal{I},k} - \bar{z}_{\mathcal{I},k}\right) \\ \bar{x}_k = A_{k-1}\hat{x}_{k-1} + B_{k-1}u_{k-1} \\ \bar{z}_{\mathcal{I},k} = D_{\mathcal{I},k}\bar{x}_k \end{cases} \tag{14}$$

where $G_{\mathcal{I},k}^L$ is the filter gain to be designed.

Then, by substituting (12) into (14), the estimation error $\tilde{x}_k = x_k - \hat{x}_k$ of KLF (14) can be expressed as

$$\tilde{x}_k = x_k - \bar{x}_k - G^L_{\mathcal{I},k}\big(0.5I + \Delta_{\mathcal{I},k}\big)\big(z_{\mathcal{I},k} - \bar{z}_{\mathcal{I},k}\big). \quad (15)$$

Obviously, due to the uncertainty $\Delta_{\mathcal{I},k}$ contained in $\tilde{x}_k$, the exact value of the estimation error covariance $\hat{P}_k = E[(x_k - \hat{x}_k)(x_k - \hat{x}_k^T)]$ cannot be obtained. Therefore, a conservative estimation error covariance $\hat{\Phi}_k$ (i.e., an upper bound of $\hat{P}_k$) that incorporates all possible values of the uncertainty will be derived and then the filter gain $G^L_{\mathcal{I},k}$ can be given by minimizing $\mathrm{Tr}(\hat{\Phi}_k)$ in Theorem 1.

Theorem 1: When $\mathcal{I}_k \neq \varnothing$, the upper bound $\hat{\Phi}_k$ of $\hat{P}_k$ that satisfies $\hat{\Phi}_k \geq \hat{P}_k$ for all Δ_k is calculated by

$$\begin{aligned}\hat{\Phi}_k = {} & 0.25G^L_{\mathcal{I},k}\big[D_{\mathcal{I},k}\Upsilon_k D^T_{\mathcal{I},k} + \beta_k I + \Xi_k\big]\big(G^L_{\mathcal{I},k}\big)^T \\ & - 0.5\Upsilon_k D^T_{\mathcal{I},k}\big(G^L_{\mathcal{I},k}\big)^T - 0.5G^L_{\mathcal{I},k}D_{\mathcal{I},k}\Upsilon_k + \Upsilon_k \end{aligned} \quad (16)$$

where α_k and β_k are the given adjustable parameters satisfying

$$\alpha_k I > \Psi_k, \quad \beta_k I > D_{\mathcal{I},k}\bar{\Phi}_k D^T_{\mathcal{I},k} \quad (17)$$

and

$$\begin{cases} \Upsilon_k \triangleq \bar{\Phi}_k + \bar{\Phi}_k D^T_{\mathcal{I},k}(\beta_k I - D_{\mathcal{I},k}\bar{\Phi}_k D^T_{\mathcal{I},k})^{-1} D_{\mathcal{I},k}\bar{\Phi}_k \\ \Xi_k \triangleq \Psi_k + \Psi_k(\alpha_k I - \Psi_k)^{-1}\Psi_k + \alpha_k I \\ \bar{\Phi}_k \triangleq A_{k-1}\hat{\Phi}_{k-1}A^T_{k-1} + C_{k-1}Q_{k-1}C^T_{k-1} \\ \Psi_k \triangleq E_{\mathcal{I},k}R_{\mathcal{I},k}E^T_{\mathcal{I},k}. \end{cases} \quad (18)$$

Meanwhile, by minimizing $\mathrm{Tr}(\hat{\Phi}_k)$, the filter gain $G^L_{\mathcal{I},k}$ is obtained by

$$G^L_{\mathcal{I},k} = 2\Upsilon^T_k D^T_{\mathcal{I},k}\big[D_{\mathcal{I},k}\Upsilon_k D^T_{\mathcal{I},k} + \beta_k I + \Xi_k\big]^{-1}. \quad (19)$$

Furthermore, by minimizing the upper bound of $\hat{\Phi}_k$ given by (16) and (19), the optimal α_k can be chosen as

$$\alpha_k = 2d_{\max}(\Psi_k). \quad (20)$$

Proof: Substituting (2), (10), and (14) into (15), one has

$$\begin{aligned}\tilde{x}_k = {} & \big[I - 0.5G^L_{\mathcal{I},k}D_{\mathcal{I},k} - 0.5G^L_{\mathcal{I},k}2\Delta_{\mathcal{I},k}D_{\mathcal{I},k}\big]A_{k-1}\tilde{x}_{k-1} \\ & + \big[I - 0.5G^L_{\mathcal{I},k}D_{\mathcal{I},k} - 0.5G^L_{\mathcal{I},k}2\Delta_{\mathcal{I},k}D_{\mathcal{I},k}\big]C_{k-1}w_{k-1} \\ & - 0.5G^L_{\mathcal{I},k}\big(I + 2\Delta_{\mathcal{I},k}\big)E_{\mathcal{I},k}v_{\mathcal{I},k}. \end{aligned} \quad (21)$$

Then, the estimation error covariance is calculated by

$$\begin{aligned}\hat{P}_k = {} & \big(I - 0.5G^L_{\mathcal{I},k}D_{\mathcal{I},k} - 0.5G^L_{\mathcal{I},k}2\Delta_{\mathcal{I},k}D_{\mathcal{I},k}\big) \\ & \times \big(A_{k-1}\hat{P}_{k-1}A^T_{k-1} + C_{k-1}Q_{k-1}C^T_{k-1}\big) \\ & \times \big(I - 0.5G^L_{\mathcal{I},k}D_{\mathcal{I},k} - 0.5G^L_{\mathcal{I},k}2\Delta_{\mathcal{I},k}D_{\mathcal{I},k}\big)^T \\ & + 0.25G^L_{\mathcal{I},k}\big(I + 2\Delta_{\mathcal{I},k}\big)\Psi_k\big(I + 2\Delta_{\mathcal{I},k}\big)^T\big(G^T_{\mathcal{I},k}\big)^L \end{aligned} \quad (22)$$

where Ψ_k is defined in (18).

Notice that $2\Delta_{\mathcal{I},k}2\Delta_{\mathcal{I},k} \leq I$ and $\hat{\Phi}_{k-1}$ are upper bounds for $\hat{P}_{k-1}$. In this case, it follows from Lemma 1 in [27] that the following inequalities hold:

$$\begin{aligned}& \big(I - 0.5G^L_{\mathcal{I},k}D_{\mathcal{I},k} - 0.5G^L_{\mathcal{I},k}2\Delta_{\mathcal{I},k}D_{\mathcal{I},k}\big) \\ & \quad \times \big(A_{k-1}\hat{P}_{k-1}A^T_{k-1} + C_{k-1}Q_{k-1}C^T_{k-1}\big) \\ & \quad \times \big(I - 0.5G^L_{\mathcal{I},k}D_{\mathcal{I},k} - 0.5G^L_{\mathcal{I},k}2\Delta_{\mathcal{I},k}D_{\mathcal{I},k}\big)^T \\ & \leq N_k\bar{\Phi}_k D^T_{\mathcal{I},k}\big(\beta_k I - D_{\mathcal{I},k}\bar{\Phi}_k D^T_{\mathcal{I},k}\big)^{-1}D_k\bar{\Phi}_k N^T_k \\ & \quad + N_k\bar{\Phi}_k N^T_k + 0.25\beta_k G^L_{\mathcal{I},k}\big(G^L_{\mathcal{I},k}\big)^T \end{aligned} \quad (23)$$

$$\begin{aligned}& 0.25G^L_{\mathcal{I},k}\big(I + 2\Delta_{\mathcal{I},k}\big)\Psi_k\big(I + 2\Delta_{\mathcal{I},k}\big)^T\big(G^L_{\mathcal{I},k}\big)^T \\ & \quad \leq 0.25G^L_{\mathcal{I},k}\big[\Psi_k + \Psi_k(\alpha_k I - \Psi_k)^{-1}\Psi_k + \alpha_k I\big]\big(G^L_{\mathcal{I},k}\big)^T \end{aligned} \quad (24)$$

where $N_k = I - 0.5G^L_{\mathcal{I},k}D_{\mathcal{I},k}$, $\bar{\Phi}_k$, is defined in (18), and α_k and β_k are the given parameters that satisfy the conditions in (17).

Substituting (23) and (24) into (22), one can deduce that $\hat{\Phi}_k \geq \hat{P}_k$ holds for all Δ_k. In this case, the optimization objective is chosen as $\mathrm{Tr}(\hat{\Phi}_k)$, and taking the partial derivative of $\mathrm{Tr}(\hat{\Phi}_k)$ with respect to $G^L_{\mathcal{I},k}$ yields that

$$\frac{\partial \mathrm{Tr}\big(\hat{\Phi}_k\big)}{\partial G^L_{\mathcal{I},k}} = -\Upsilon^T_k D^T_{\mathcal{I},k} + 0.5G^L_{\mathcal{I},k}\big[D_{\mathcal{I},k}\Upsilon_k D^T_{\mathcal{I},k} + \beta_k I + \Xi_k\big]$$

where Υ_k and Ξ_k are defined in (18). Let $\partial\mathrm{Tr}(\hat{\Phi}_k)/\partial G^L_{\mathcal{I},k}$ equal to O, the filter gain $G^L_{\mathcal{I},k}$ can be obtained from (19).

Next, an optimal way of selecting α_k will be given by minimizing the upper bound of $\hat{\Phi}_k$. Substituting (19) into (16), $\hat{\Phi}_k$ is rearranged into

$$\hat{\Phi}_k = \Upsilon_k - \Upsilon_k D^T_{\mathcal{I},k}\big(D_{\mathcal{I},k}\Upsilon_k D^T_{\mathcal{I},k} + \beta_k I + \Xi_k\big)^{-1}D_{\mathcal{I},k}\Upsilon_k.$$

Notice that Ξ_k is a diagonal matrix, and thus one has

$$\begin{aligned}\hat{\Phi}_k \leq {} & -\Upsilon_k D^T_{\mathcal{I},k}\big(D_{\mathcal{I},k}\Upsilon_k D^T_{\mathcal{I},k} + \beta_k I + d_{\max}(\Xi_k)I\big)^{-1}D_{\mathcal{I},k} \\ & \times\Upsilon_k + \Upsilon_k. \end{aligned}$$

Obviously, only the matrix Ξ_k contains the parameter α_k. Then, to minimize the upper bound of $\hat{\Phi}_k$, the objective function should be

$$\begin{cases} \min\limits_{\alpha_k} d_{\max}(\Xi_k) \\ \text{s.t. } \alpha_k I > \Psi_k. \end{cases} \quad (25)$$

To solve (25), the maximum diagonal element of Ξ_k needs to be determined. Then, it follows from the definition of Ξ_k in (18) that

$$d_i(\Xi_k) = d_i(\Psi_k) + \frac{d_i^2(\Psi_k)}{\alpha_k - d_i(\Psi_k)} + \alpha_k, \quad i = 1, 2, \ldots, m_k.$$

Taking the partial derivative of $d_i(\Xi_k)$ with respect to $d_i(\Psi_k)$, one has

$$\frac{\partial d_i(\Xi_k)}{\partial d_i(\Psi_k)} = 1 + \frac{d_i(\Psi_k)(2\alpha_k - d_i(\Psi_k))}{(\alpha_k - d_i(\Psi_k))^2}.$$

Then, notice that the constraint in (25) is equivalent to $\alpha_k > d_{\max}(\Psi_k)$ in which case the above equation is greater than 0. Thus, we can know that $d_i(\Xi_k)$ increases as $d_i(\Psi_k)$ increases when α_k is invariable. In this case, one can deduce that

$$d_{\max}(\Xi_k) = d_{\max}(\Psi_k) + \frac{d^2_{\max}(\Psi_k)}{\alpha_k - d_{\max}(\Psi_k)} + \alpha_k.$$

Finally, by taking the derivative of $d_{\max}(\Xi_k)$ with respect to α_k and making it equal to 0, the analytical solution of (25) can be obtained from (20). The proof is completed. □

When $\mathcal{I}_k = \varnothing$, no innovations are included in the binary measurements, and thus the state estimate is equal to the one-step prediction

$$\hat{x}_k = \bar{x}_k = A_{k-1}\hat{x}_{k-1} + B_{k-1}u_{k-1}, \quad \mathcal{I}_k = \varnothing. \tag{26}$$

In this case, one has

$$\begin{aligned}\hat{P}_k &= E\big[(x_k - \bar{x}_k)(x_k - \bar{x}_k)^T\big] \\ &\le A_{k-1}\hat{\Phi}_{k-1}A_{k-1}^T + C_{k-1}Q_{k-1}C_{k-1}^T \\ &= \bar{\Phi}_k, \quad \mathcal{I}_k = \varnothing.\end{aligned} \tag{27}$$

Through the analysis in this section, the computation procedures for linear binary Kalman-like filter (LBKLF) can be summarized by Algorithm 1.

Algorithm 1 Linear Binary Kalman-Like Filter

1: Initialize: $k = 0$, $\hat{x}_0$, $\hat{\Phi}_0$, τ^i, $i = 1, 2, \ldots, m$;
2: Input: $\hat{x}_{k-1}$, $\hat{\Phi}_{k-1}$ and y_k^i, $i = 1, 2, \ldots, m$;
3: Calculate $\bar{x}_k$ and $\bar{\Phi}_k$ by (9) and (18);
4: Calculate $\bar{z}_k^i$ and $\bar{y}_k^i$, $i = 1, 2, \ldots, m$ by (8) and (3);
5: Determine $\mathcal{I}_k$ by (5);
6: **if** $\mathcal{I}_k \neq \varnothing$ **then**
7: Calculate α_k by (20);
8: Determine β_k by experience;
9: Calculate filter gain $G_{\mathcal{I},k}^L$ by (19);
10: Calculate the state estimate $\hat{x}_k$ and conservative estimation error covariance $\hat{\Phi}_k$ by (14) and (16), respectively;
11: **else**
12: $\hat{x}_k = \bar{x}_k$, $\hat{\Phi}_k = \bar{\Phi}_k$;
13: **end if**
14: $k \leftarrow k + 1$ and return to step 2.

Remark 3: The relationship between $\hat{\Phi}_k$ and β_k is complex, which makes it difficult to find an optimal explicit expression for β_k. However, it can be known from (19) that when β_k is sufficient large, the gain $G_{\mathcal{I},k}^L$ will tend to be O. Moreover, one can see from (14) that the state estimate $\hat{x}_k$ is equal to the weighted fusion of the one-step prediction and the innovation (measurement information). Therefore, when the measurement information is inaccurate, the gain $G_{\mathcal{I},k}^L$ should be small and vice versa. This fact inspires us that, when choosing β_k, the precision of the measurement information should be taken into account. Specifically, when R_k^i is large or the signal-to-noise ratio of z_k^i is low, β_k should be chosen larger to reduce the contribution of the measurement information in the filter, and β_k should be chosen smaller otherwise.

B. KLF for Nonlinear Systems With Binary Sensors

In this section, we discuss the design method of KLF for the nonlinear dynamic system (1). Since both the state x_k and sensed variable z_k^i of system (1) are nonlinear, the one-step predictions cannot be obtained directly by linear transformations as in the previous section. A common way to deal with the above nonlinearity is linearizing $f(\cdot)$ and $h^i(\cdot)$ by using Taylor first-order expansion which is however only applicable to differentiable and low nonlinear systems. In contrast, the unscented transform (UT) [3] calculates the statistical properties of the random variables through a specific set of sampling points, which is applicable to arbitrary nonlinear systems and performs well with moderate nonlinearity. Based on this fact, the UT is adopted in this article.

For system (1), the one-step state prediction $\bar{x}_k$, error covariance $\bar{P}_k = E[(x_k - \bar{x}_k)(x_k - \bar{x}_k)^T]$, and one-step prediction $\bar{z}_k^i$ of sensed variable z_k^i can be calculated by using UT

$$\bar{x}_k = \sum_{j=0}^{2n} w_j^m f\big(\hat{\chi}_{k-1,j}, u_{k-1}\big) \tag{28}$$

$$\begin{aligned}\bar{P}_k = &\sum_{j=0}^{2n} w_j^c \big(f\big(\hat{\chi}_{k-1,j}, u_{k-1}\big) - \bar{x}_k\big)\big(f\big(\hat{\chi}_{k-1,j}, u_{k-1}\big) - \bar{x}_k\big)^T \\ &+ C_{k-1}Q_kC_{k-1}^T\end{aligned} \tag{29}$$

$$\bar{z}_k^i = \sum_{j=0}^{2n} w_j^m h^i\big(\bar{\chi}_{k,j}\big), \quad i = 1, 2, \ldots, m \tag{30}$$

where w_j^m and w_j^c are the weights in the UT, $\hat{\chi}_{k-1,j}$ and $\bar{\chi}_{k,j}$ are the sigma points in the UT, and their specific expressions are presented in Appendix. Then, according to (3), (5), and (30), $\mathcal{I}_k$ can be determined.

When $\mathcal{I}_k = \varnothing$, the state estimate $\hat{x}_k$ and conservative estimation error covariance $\hat{\Phi}_k$ are equal to the one-step predictions

$$\hat{x}_k = \bar{x}_k, \quad \hat{\Phi}_k = \bar{P}_k, \quad \mathcal{I}_k = \varnothing.$$

When $\mathcal{I}_k \neq \varnothing$, similar to the previous section, augmenting the binary measurements that belong to $\mathcal{I}_k$, one has

$$\begin{aligned}z_{\mathcal{I},k} &= h_{\mathcal{I},k}(x_k) + E_{\mathcal{I},k}v_{\mathcal{I},k} \\ \bar{z}_{\mathcal{I},k} &= \sum_{j=0}^{2n} w_j^m h_{\mathcal{I},k}\big(\bar{\chi}_{k,j}\big) \\ \tau_{\mathcal{I},k} &= \big(0.5I - \Delta_{\mathcal{I},k}\big)\bar{z}_{\mathcal{I},k} + \big(0.5I + \Delta_{\mathcal{I},k}\big)z_{\mathcal{I},k}\end{aligned} \tag{31}$$

where $h_{\mathcal{I},k}(\cdot)$ is defined in (7). Then, the one-step prediction of (31) can also be given by

$$\bar{\tau}_{\mathcal{I},k} = \big(0.5I - \Delta_{\mathcal{I},k}\big)\bar{z}_{\mathcal{I},k} + \big(0.5I + \Delta_{\mathcal{I},k}\big)\bar{z}_{\mathcal{I},k} = \bar{z}_{\mathcal{I},k}. \tag{32}$$

Thus, the nonlinear KLF can be constructed for system (1)

$$\begin{cases}\hat{x}_k = \bar{x}_k + G_{\mathcal{I},k}^N\big(\tau_{\mathcal{I},k} - \bar{z}_{\mathcal{I},k}\big) \\ \bar{x}_k = \displaystyle\sum_{j=0}^{2n} w_j^m f\big(\hat{\chi}_{k-1,j}, u_{k-1}\big) \\ \bar{z}_{\mathcal{I},k} = \displaystyle\sum_{j=0}^{2n} w_j^m h_{\mathcal{I},k}\big(\bar{\chi}_{k,j}\big)\end{cases} \tag{33}$$

where $G_{\mathcal{I},k}^N$ is the filter gain that will be designed in the Theorem 2.

Theorem 2: When $\mathcal{I}_k \neq \varnothing$, the conservative estimation error covariance $\hat{\Phi}_k$ of the KLF (33) that incorporates all possible

values of the uncertainty $\Delta_{\mathcal{I},k}$ is calculated by

$$\begin{aligned}\hat{\Phi}_k = \bar{P}_k &- 0.5\bar{P}_k^{xz}\left(G_{\mathcal{I},k}^N\right)^T - 0.5G_{\mathcal{I},k}^N\left(\bar{P}_k^{xz}\right)^T \\ &+ 0.25G_{\mathcal{I},k}^N\Big[\bar{P}_k^{zz} + \bar{P}_k^{zz}\left(\varepsilon_k I - \bar{P}_k^{zz}\right)^{-1}\bar{P}_k^{zz} \\ &+ (\varepsilon_k + \xi_k)I\Big]\left(G_{\mathcal{I},k}^N\right)^T + \frac{1}{\xi_k}\bar{P}_k^{xz}\left(\bar{P}_k^{xz}\right)^T\end{aligned} \tag{34}$$

where ε_k and ξ_k are given adjustable parameters satisfying

$$\varepsilon_k I > \bar{P}_k^{zz}, \quad \xi_k > 0 \tag{35}$$

and

$$\bar{P}_k^{xz} = \sum_{j=0}^{2n} w_j^c\left(\bar{\chi}_{k,j} - \bar{x}_k\right)\left(h_{\mathcal{I},k}\left(\bar{\chi}_{k,j}\right) - \bar{z}_{\mathcal{I},k}\right)^T \tag{36}$$

$$\begin{aligned}\bar{P}_k^{zz} = &\sum_{j=0}^{2n} w_j^c\left(h_{\mathcal{I},k}\left(\bar{\chi}_{k,j}\right) - \bar{z}_{\mathcal{I},k}\right)\left(h_{\mathcal{I},k}\left(\bar{\chi}_{k,j}\right) - \bar{z}_{\mathcal{I},k}\right)^T \\ &+ E_k R_k E_k^T.\end{aligned} \tag{37}$$

Meanwhile, by minimizing $\mathrm{Tr}(\hat{\Phi}_k)$, the nonlinear filter gain $G_{\mathcal{I},k}^N$ can be obtained by

$$G_{\mathcal{I},k}^N = 2\bar{P}_k^{xz}\Big[\bar{P}_k^{zz} + \bar{P}_k^{zz}\left(\varepsilon_k I - \bar{P}_k^{zz}\right)^{-1}\bar{P}_k^{zz} + (\varepsilon_k + \xi_k)I\Big]^{-1}. \tag{38}$$

Furthermore, when minimizing the upper bound of the $\hat{\Phi}_k$ given by (34) and (38), the optimal ε_k is chosen as

$$\varepsilon_k = 2\lambda_{\max}\left(\bar{P}_k^{zz}\right). \tag{39}$$

Proof: Substituting (31) into (33), the estimate error $\tilde{x}_k = x_k - \hat{x}_k$ is given by

$$\tilde{x}_k = x_k - \bar{x}_k - G_{\mathcal{I},k}^N\left(0.5 + \Delta_{\mathcal{I},k}\right)\left(z_{\mathcal{I},k} - \bar{z}_{\mathcal{I},k}\right).$$

Then, the estimation error covariance is calculated by

$$\begin{aligned}\hat{P}_k = \bar{P}_k &- 0.5\bar{P}_k^{xz}\left(I + 2\Delta_{\mathcal{I},k}\right)\left(G_{\mathcal{I},k}^N\right)^T \\ &- 0.5G_{\mathcal{I},k}^N\left(I + 2\Delta_{\mathcal{I},k}\right)\left(\bar{P}_k^{xz}\right)^T \\ &+ 0.25G_{\mathcal{I},k}^N\left(I + 2\Delta_{\mathcal{I},k}\right)\bar{P}_k^{zz}\left(I + 2\Delta_{\mathcal{I},k}\right)\left(G_{\mathcal{I},k}^N\right)^T\end{aligned} \tag{40}$$

where the expressions for $\bar{P}_k^{xz} = E[(x_k - \bar{x}_k)(z_k - \bar{z}_k)^T]$ and $\bar{P}_k^{zz} = E[(z_k - \bar{z}_k)(z_k - \bar{z}_k)^T]$ can be given by using UT as shown in (36) and (37), respectively.

Using Lemma 1 in [27], one has

$$\begin{aligned}&G_{\mathcal{I},k}^N\left(I + 2\Delta_{\mathcal{I},k}\right)\bar{P}_k^{zz}\left(I + 2\Delta_{\mathcal{I},k}\right)\left(G_{\mathcal{I},k}^N\right)^T \\ &\le G_{\mathcal{I},k}^N\Big[\bar{P}_k^{zz} + \bar{P}_k^{zz}\left(\varepsilon_k I - \bar{P}_k^{zz}\right)^{-1}\bar{P}_k^{zz} + \varepsilon_k I\Big]\left(G_{\mathcal{I},k}^N\right)^T.\end{aligned} \tag{41}$$

Moreover, it follows from Lemma 2.2 in [30] that

$$\begin{aligned}-\bar{P}_k^{xz}\Delta_{\mathcal{I},k}\left(G_{\mathcal{I},k}^N\right)^T &- \left(G_{\mathcal{I},k}^N\right)^T\Delta_{\mathcal{I},k}\left(\bar{P}_k^{xz}\right)^T \\ &\le 0.25\xi_k G_{\mathcal{I},k}^N\left(G_{\mathcal{I},k}^N\right)^T + \frac{1}{\xi_k}\bar{P}_k^{xz}\left(\bar{P}_k^{xz}\right)^T\end{aligned} \tag{42}$$

where ε_k and ξ_k are given adjustable parameters that satisfy the conditions in (35). Then, substituting (41) and (42) into (40), we know that $\hat{\Phi}_k \ge \hat{P}_k$ holds for all Δ_k, where the expression of $\hat{\Phi}_k$ is shown in (34). In this case, $\hat{\Phi}_k$ can be seen as a conservative estimation error covariance of the KLF (33), and the effect of the approximation error caused by UT can also be included in $\hat{\Phi}_k$.

Then, calculating $\partial\mathrm{Tr}(\hat{\Phi}_k)/\partial G_{\mathcal{I},k}^N$ and make it equal to O, the nonlinear filter gain $G_{\mathcal{I},k}^N$ is given by (38).

Substituting (38) into (34), $\hat{\Phi}_k$ is rearranged into

$$\begin{aligned}\hat{\Phi}_k = \bar{P}_k - \bar{P}_k^{xz}\left[\bar{P}_k^{zz} + M(\varepsilon_k) + \xi_k I\right]^{-1}\left(\bar{P}_k^{xz}\right)^T \\ + \frac{1}{\xi_k}\bar{P}_k^{xz}\left(\bar{P}_k^{xz}\right)^T\end{aligned} \tag{43}$$

where $M(\varepsilon_k) = \bar{P}_k^{zz}(\varepsilon_k I - \bar{P}_k^{zz})^{-1}\bar{P}_k^{zz} + \varepsilon_k I$ represents the terms associated with ε_k. Obviously, for (43), the following inequality holds:

$$\begin{aligned}\hat{\Phi}_k \le \bar{P}_k - \bar{P}_k^{xz}\left[\bar{P}_k^{zz} + \lambda_{\max}(M(\varepsilon_k))I + \xi_k I\right]^{-1}\left(\bar{P}_k^{xz}\right)^T \\ + \frac{1}{\xi_k}\bar{P}_k^{xz}\bar{P}_k^{xz}.\end{aligned}$$

Thus, to minimize the upper bound of $\hat{\Phi}_k$, the objective function should be

$$\begin{cases}\min\limits_{\varepsilon_k}\lambda_{\max}(M(\varepsilon_k)) \\ \text{s.t. } \varepsilon_k I > \bar{P}_k^{zz}.\end{cases} \tag{44}$$

Using the basic properties of matrix eigenvalues, it is not difficult to prove that the eigenvalues of $M(\varepsilon_k)$ are

$$\lambda_i(M(\varepsilon_k)) = \frac{\lambda_i^2\left(\bar{P}_k^{zz}\right)}{\varepsilon_k - \lambda_i\left(\bar{P}_k^{zz}\right)} + \varepsilon_k, \quad i = 1, 2, \ldots, m_k.$$

Finally, using the similar approach as for solving (25) in Theorem 1, the analytic solution of (44) can be obtained from (39). The proof is completed. □

According to the analysis in this section, the computation procedures for nonlinear binary Kalman-like filter (NBKLF) are summarized by Algorithm 2. Furthermore, an algorithm flowchart is also provided in Fig. 2, which contains the main steps of the proposed LBKLF and NBKLF.

Algorithm 2 Nonlinear Binary Kalman-Like Filter

1: Initialize: $k = 0$, $\hat{x}_0$, $\hat{\Phi}_0$, τ^i, $i = 1, 2, \ldots, L$;
2: Input: $\hat{x}_{k-1}$, Φ_{k-1} and y_k^i, $i = 1, 2, \ldots, L$;
3: Calculate $\bar{x}_k$ and $\bar{P}_k$ by (28) and (29), respectively;
4: Calculate $\bar{z}_k^i$ and $\bar{y}_k^i$ $i = 1, 2, \ldots, L$ by (30) and (3);
5: Determine $\mathcal{I}_k$ by (5);
6: **if** $\mathcal{I}_k \neq \varnothing$ **then**
7: Calculate ε_k by (39);
8: Determine ξ_k by experience;
9: Calculate nonlinear filter Gain $G_{\mathcal{I},k}^N$ by (38);
10: Calculate the state estimate $\hat{x}_k$ and conservative estimation error covariance $\hat{\Phi}_k$ by (33) and (34), respectively;
11: **else**
12: $\hat{x}_k = \bar{x}_k$, $\hat{\Phi}_k = \bar{\Phi}_k$;
13: **end if**
14: $k \leftarrow k + 1$ and return to step 2;

Remark 4: Notice that, Lemma 1 in [27] and Lemma 2.2 in [30] are two matrix inequalities that commonly used to deal with the uncertainty, but the adoption of these two

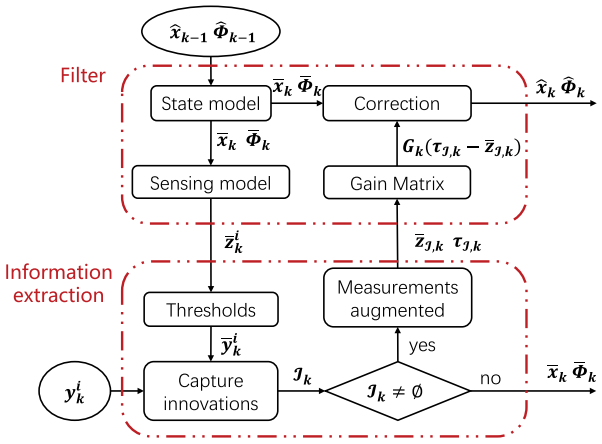

Fig. 2. Main steps of the proposed LBKLF and NBKLF.

matrix inequalities necessarily introduces adjustable parameters which are often chosen empirically in most literatures. In fact, experience is sometimes unreliable. Therefore, to reduce the influence of experience on the filter as much as possible, an optimal selection of the adjustable parameters α_k and ε_k are given by minimizing the upper bound of $\hat{\Phi}_k$ in this article. However, the DFKLF in [27] does not take this into account, although similar adjustable parameters also exist in it.

Remark 5: When constructing KLF based on (6), one-step prediction of (6) needs to be calculated

$$\bar{\tau}^i = \left(0.5 - \epsilon_k^i\right)\hat{z}_{k-1}^i + \left(0.5 + \epsilon_k^i\right)\bar{z}_k^i, \quad i \in \mathcal{S}_k \tag{45}$$

where $\hat{z}_{k-1}$ is the estimation of z_{k-1}, and it is obtained from $\hat{x}_{k-1}$ and the measurement equations. Unfortunately, due to uncertainty ϵ_k^i, the exact value of $\bar{\tau}^i$ is unknown. Thus, ϵ_k^i has to be ignored, and then the following KLF can be constructed for single binary sensor [27], [28]:

$$\hat{x}_k = \bar{x}_k + G_k^i\left(\tau^i - 0.5\hat{z}_{k-1}^i - 0.5\bar{z}_k^i\right). \tag{46}$$

The formula (46) is the structure of KLFs in [27] and [28]. Obviously, their estimation performance is reduced because ϵ_k^i is ignored. In addition, the uncertainties caused by the binary sensors were also ignored in [26] when constructing the moving horizon estimator, and the specific analysis of this can be found in Remark 1 of [28]. In contrast, benefiting from the form of innovation-based model (4), the uncertainty $\Delta_{\mathcal{I},k}$ is offset rather than ignored when calculating $\bar{\tau}_{\mathcal{I},k}$ in (13) and (32). In this case, LBKLF and NBKLF have better estimation performance than the methods in [26]–[28].

Remark 6: The algorithms proposed in this article take centralized approach, that is, augmenting the measurements. However, it follows from (7) that only those binary measurements containing innovations are augmented. In this case, the computational complexity of LBKLF and NBKLF are $O(n^3 + n^2 m_k + n m_k^2 + m_k^3)$, where m_k represents the number of binary measurements contained in the set $\mathcal{I}_k$. Obviously, the computational complexity of the proposed algorithms is not directly related to the total number of binary sensors m, but it is related to m_k which is less than m. Therefore, the proposed algorithms overcome the disadvantage that the computational complexity of traditional centralized approach increases sharply when the number of sensors increasing.

IV. Simulation Results

A. O_2 Content Estimation in Arteries

Consider arterial O_2 content estimation using the noninvasive binary pulmonary sensors where the physiological model for the arterial O_2 content is [27]

$$\begin{aligned} x_{k+1} &= f x_k + U_k + w_k \\ U_k &= (1-f)(1.34\mathrm{Hb} + 0.003(a u_k + c_k e_k)) - f\mu \\ a &= P_{\mathrm{ATM}} - P_{\mathrm{H_2O}} \\ c_k &= [1 - u_k(1 - \mathrm{RQ})]/\mathrm{RQ} \end{aligned}$$

where x_k is the arterial O_2 content, u_k is the percentage of O_2 in the inhaled air and is set by surgeons, and thus it can be considered as the control input. f represents the fraction of shunted blood. e_k is the partial pressure of exhaled CO_2 and can be measured directly. Hb is the amount of hemoglobin, P_{ATM} and $P_{\mathrm{H_2O}}$ are the atmospheric and water vapor pressures, respectively, μ reflects the patient-specific metabolic rate, and RQ is the respiratory quotient. Specifically, to ensure that the simulation is meaningful, the above parameters are chosen to be the per capita levels provided in the medical literature [32]: Hb = 12 g/dL, $P_{\mathrm{ATM}} = 760$ mmHg, $P_{\mathrm{H_2O}} = 47$ mmHg, $\mu = 5$ mL/dL, and RQ = 0.8. Moreover, $f = 0.75$ and u_k is set to 60%. Meanwhile, the sensed variable z_k^i is constructed by three other inputs: tidal volume, respiratory rate, and peak inspiratory, and it is proportional to the O_2 content [32]

$$z_k^i = D_k^i x_k + v_k^i, \quad i = 1, 2, \ldots, L.$$

where $D_k^i = 0.5$, $i = 1, 2, \ldots, L$. w_k and v_k^i are white noise with covariance $(1\ \mathrm{mL/dL})^2$ and R_k^i, respectively. Here, the O_2 content change process is monitored by 10 binary sensors and their thresholds are set to $\tau^i = 61 + 0.5i$, $i = 1, 2, \ldots, 10$.

First, the relationship between the adjustable parameter β_k and the estimation performance of LBKLF will be analyzed. Due to the random noises, the estimation performance is assessed by the root mean square error (RMSE), and 100 MC runs are implemented to approximate the ideal RMSE. Then, the relationship between R_k^i and optimal β_k is shown in Fig. 3, from which we can see that the optimal β_k is generally increasing as R_k^i increases. Here, the optimal β_k denotes the β_k that minimizes RMSE of LBKLF. In fact, this is consistent with our analysis in Remark 3, that is, when the measurement is imprecise, β_k should become larger to reduce the contribution of the measurement in the filter.

Notice that searching for the optimal β_k is not always convenient in practice. Therefore, to be fair, β_k is not chosen as the optimal value in subsequent simulations, but is chosen uniformly as $1.5\lambda_{\max}(D_{\mathcal{I},k}\bar{\Phi}_k D_{\mathcal{I},k}^T)$. Then, by implementing Algorithm 1, the trajectories of true arterial O_2 content and the estimated arterial O_2 content by using the LBKLF are plotted in Fig. 4, which shows that the proposed LBKLF can estimate the arterial O_2 content well. Moreover, to highlight the advantages of the proposed LBKLF, we compare it with DFKLF in [27] and MHE in [26], where the sliding window

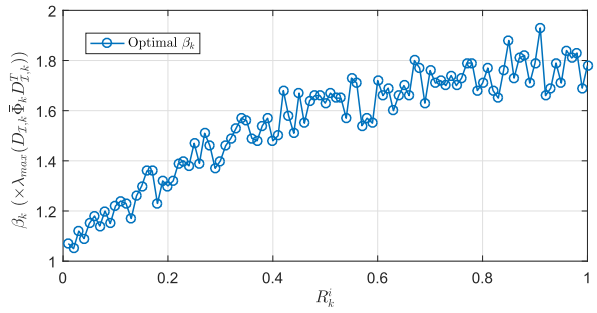

Fig. 3. Optimal value of adjustable parameter β_k in Algorithm 1 when $R_k^i \in [0.01, 1]$.

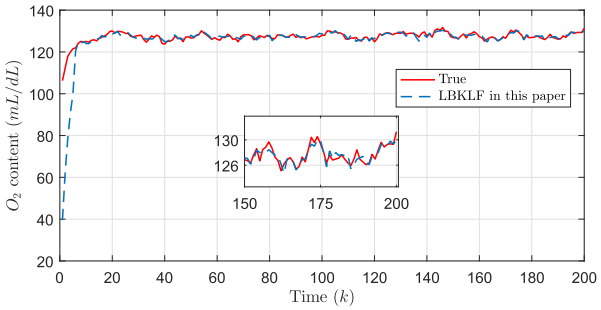

Fig. 4. True O_2 content and the estimated O_2 content by using LBKLF when $R_k^i = 0.5$.

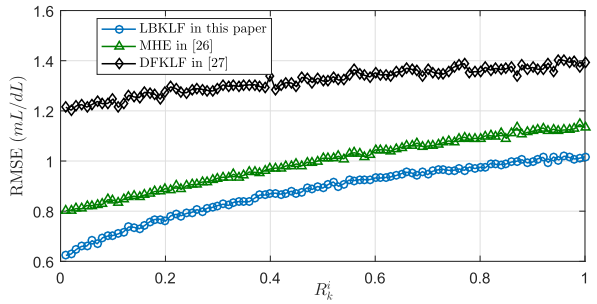

Fig. 5. Comparisons of the O_2 content RMSEs of the LBKLF in this article, DFKLF in [27] and MHE in [26] when $R_k^i \in [0.01, 1]$.

size for the MHE is chosen to be 50 and the fusion criterion for DFKLF is chosen to be fast covariance intersection fusion [31]. Furthermore, in order to provide comprehensive simulation as possible, 100 different measurement covariances R_k^i will be considered. Then, the RMSEs of LBKLF, DFKLF in [27], and MHE in [26] for different R_k^i are plotted in Fig. 5, from which we can see that the estimation accuracy of the LBKLF is always higher than that of DFKLF and MHE, which is mainly caused by three factors: 1) the uncertainties caused by the binary sensors are offset in LBKLF, rather than ignored directly as in DFKLF and MHE; 2) compared with the switch-based model in [26] and [27], the proposed innovation-based model (4) can capture more innovations which play a major role in the filer; and 3) Compared with the DFKLF, the proposed LBKLF gives an optimal selection criterion for the adjustable parameter α_k and thus reducing the unreliability caused by experience. Moreover, it is important to emphasize that β_k is not set to be optimal, which means that the simulation result in Fig. 5 is conservative.

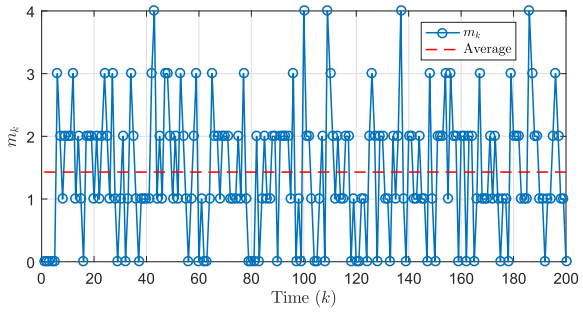

Fig. 6. Number of binary sensors m_k belonging to $\mathcal{I}_k$ when $R_k^i = 0.5$.

TABLE II
AVERAGE COMPUTATION OVERHEAD PER MOMENT OF THE LBKLF IN THIS ARTICLE, DFKLF IN [27], AND MHE IN [26]

Algorithms	LBKLF	DFKLF	MHE
Computational overhead (10^{-5}s)	3.0	27.1	40.1

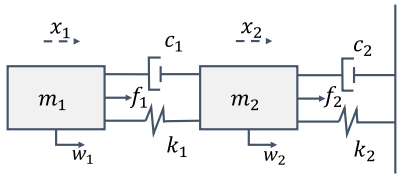

Fig. 7. Graphical representation of the DMS system.

In addition, computational efficiency is also an important criterion for assessing the merits of a filter. Then, Fig. 6 shows the number of binary sensors m_k in set $\mathcal{I}_k$. It can be seen from Fig. 6 that m_k is much smaller than the total number of binary sensors $m = 10$, and combining this fact with Remark 6 means that the computational complexity of LBKLF is low. Meanwhile, to show this point more intuitively, the computational overheads of different methods are listed in Table II, from which we can see that the LBKLF is more computationally efficient than DFKLF and MHE.

B. Damped Mass-Spring System

Consider the damped mass-spring (DMS) system shown in Fig. 7, which has wide application in mechanical design. By using Newton's second law, the differential equations for the DMS system can be written as

$$\begin{aligned} m_1\ddot{x}_1(t) &= -k_1(x_1(t) - x_2(t)) - c_1(\dot{x}_1(t) - \dot{x}_2(t)) \\ &\quad + f_1(t) + w_1(t) \\ m_2\ddot{x}_2(t) &= k_1(x_1(t) - x_2(t)) + c_1(\dot{x}_1(t) - \dot{x}_2(t)) \\ &\quad - k_2x_2(t) - c_2\dot{x}_2(t) + f_2(t) + w_2(t) \end{aligned}$$

where $x_i(t)$, $\dot{x}_i(t)$, and $\ddot{x}_i(t)$ represent the displacement, velocity, and acceleration of the ith $(i = 1, 2)$ object, respectively. m_i represents the mass of the ith object, and k_i and c_i are, respectively, the ith spring factor and damping factor. $f_1(t)$ and $f_2(t)$ are system inputs. $w_1(t)$ and $w_2(t)$ are white noise with covariance $(1\ \text{m})^2$. In this simulation, the parameters are chosen as: $m_1 = 1$ kg, $m_2 = 2$ kg, $c_1 = c_2 = 5$ N/(m/s), $k_1 = 20$ N/m, and $k_2 = 1$ N/m. Moreover, the system inputs $f_1(t) = 5\sin(t/50)$N and $f_2(t) = 0$. Two binary distance

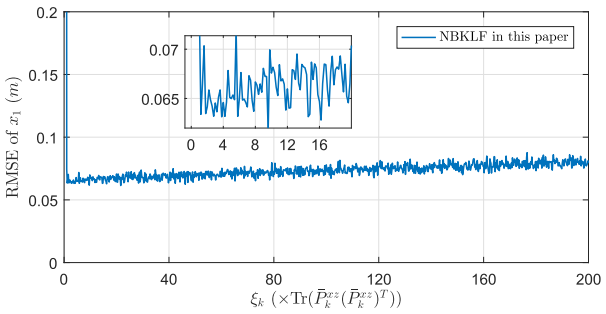

Fig. 8. Relationship between the adjustable parameter ξ_k and the RMSE of x_1 by using NBKLF.

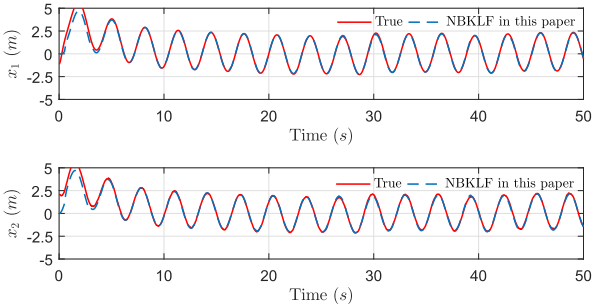

Fig. 9. True displacements and the estimated displacements by using NBKLF.

sensors are deployed here to observe the motion of object 1, and their sensing equations are

$$z_k^i = \sqrt{1 + \left(5 + x_{1,k}\right)^2} + v_k^i, \quad i = 1, 2$$

where v_k^i is the white noise with covariance $(0.1\ \mathrm{m})^2$, and $x_{1,k}$ denotes the displacement of object 1 after the DMS system is discretized with the period of $T = 0.01$ s. Meanwhile, their thresholds are set to $\tau^1 = (1 + 3.5^2)^{1/2}$ and $\tau^2 = (1 + 6.5^2)^{1/2}$.

Fig. 8 shows the RMSE of state x_1 when taking ξ_k in Algorithm 2 to be $b\mathrm{Tr}(\bar{P}_k^{xz}(\bar{P}_k^{xz})^T)$, where b is a positive number. It can be seen that the optimal ξ_k is taken roughly in the interval $[2\mathrm{Tr}(\bar{P}_k^{xz}(\bar{P}_k^{xz})^T), 10\mathrm{Tr}(\bar{P}_k^{xz}(\bar{P}_k^{xz})^T)]$. Furthermore, a noteworthy phenomenon is that the RMSE curve increases steeply as ξ_k tends to 0. In fact, this is because $\xi_k \to 0$ will cause $1/\xi_k \to \infty$, in which case NBKLF will even not work. On the other hand, when $\xi_k > 2\mathrm{Tr}(\bar{P}_k^{xz}(\bar{P}_k^{xz})^T)$, the RMSE curve generally tends to increase, but it is important to emphasize that the growth rate is slow. The two phenomena above give us guidance for selecting ξ_k: in the absence of sufficient prior knowledge that can be provided, ξ_k is suggested to be chosen larger. This is a conservative approach, and although a little estimation performance may be sacrificed, the filter will be guaranteed to work properly. In the later simulations, we set ξ_k to $15\mathrm{Tr}(\bar{P}_k^{xz}(\bar{P}_k^{xz})^T)$.

Fig. 9 shows the real displacements and the estimated displacements by using NBKLF, from which we can see that even though only two binary sensors are employed, the NBKLF still can estimate the motion of the DMS system well. Note that the sensing equations are nonlinear and thus the MHE and the DFKLF are no longer applicable. To show the effectiveness of

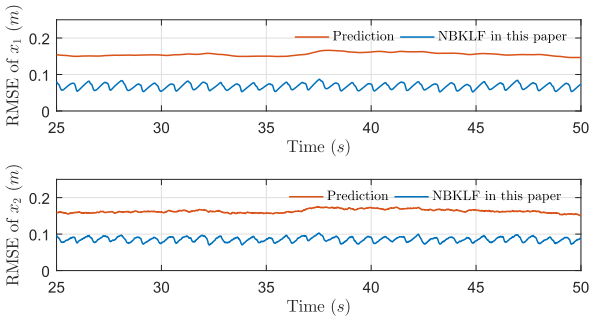

Fig. 10. Comparisons of the displacement RMSEs of the model prediction and the NBKLF in this article.

NBKLF, we present the RMSEs of model prediction method and NBKLF in Fig. 10. Here, the model prediction method is used as a benchmark, which corresponds to the case where the filter gain $G_{\mathcal{I},k}^N$ is set to O (no measurement information is used at all). Generally speaking, if the RMSE of a filter is greater than or very close to the prediction RMSE, then the filter is considered to be invalid. Then, as we can see in Fig. 10, RMSE of NBKLF is significantly smaller than the predicted RMSE. This fact verifies that NBKLF makes effective use of the information in the binary sensors. Particularly, since only two binary sensors are employed, the computational effort of NBKLF is maintained at a low level, about 6.6×10^{-5} s per recursion.

V. Conclusion

This article considered the state estimation problem for the binary sensors system. A novel innovation-based model was proposed to capture information in the binary outputs. Compared with the existing switch-based model, the novel model captured more information that is useful for the filter. Linear and nonlinear KLFs were constructed based on the innovation-based model, and the corresponding filter gains were designed by minimizing the upper bound on their mean square error. Particularly, we demonstrated that the proposed methods could ensure the estimation performance while requiring few computational resources. The effectiveness and advantages of the proposed methods were verified by the arterial O_2 system and the DMS system. In the future, analyzing the game relationship between the number of binary sensors and the estimation performance will be our main focus. Moreover, we are also interested in designing controller for the binary sensors system, which is a challenging and practically relevant problem.

Appendix

For system (1), the sampling strategy of $\hat{\chi}_{k-1,j}$ is

$$\hat{\chi}_{k-1,j} = \hat{\sigma}_{k-1,j} + \hat{x}_{k-1}, \quad j = 0, 1, \ldots, 2n$$

$$\hat{\sigma}_{k-1,j} = \begin{cases} O, & j = 0 \\ -\left(\sqrt{(n+\eta)\hat{\Phi}_{k-1}}\right)_j, & j = 1, 2, \ldots, n \\ \left(\sqrt{(n+\eta)\hat{\Phi}_{k-1}}\right)_{j-n}, & j = n+1, n+2, \ldots, 2n \end{cases}$$

where $\sqrt{A}$ denotes the Cholesky decomposition of a positive definition matrix A. Then, the predictions $\bar{x}_k$ and $\bar{P}_k$ can be computed as in (27) and (28), respectively. The sigma point $\bar{\chi}_{k,j}$ is given by

$$\bar{\chi}_{k,j} = \bar{\sigma}_{k,j} + \bar{x}_k, \quad j = 0, 1, \ldots, 2n$$

$$\bar{\sigma}_{k,j} = \begin{cases} O, & j = 0 \\ -\left(\sqrt{(n+\eta)\bar{P}_k}\right)_j, & j = 1, 2, \ldots, n \\ \left(\sqrt{(n+\eta)\bar{P}_k}\right)_{j-n}, & j = n+1, n+2, \ldots, 2n. \end{cases}$$

Moreover, the weights w_j^m and w_j^c are given by

$$\begin{cases} w_j^m = w_j^c = \dfrac{1}{2(n+\eta)}, & j = 1, 2, \ldots, 2n, \\ w_0^c = w_0^m + \left(1 - a^2 + b\right), & w_0^m = \dfrac{1}{n+\eta} \end{cases}$$

where the constants are chosen as $\eta = a^2(n+\kappa) - n$, $b = 2$, $\kappa = 0$, and $a = 1$. The principle of the UT can be referred to [3], which will not be repeated here.

REFERENCES

[1] R. E. Kalman, "A new approach to linear filtering and prediction problems," *J. Basic Eng.*, vol. 82, no. 1, pp. 34–45, Mar. 1960.

[2] A. Gelb, Ed., *Applied Optimal Estimation*. Cambridge, MA, USA: MIT Press, 1974.

[3] S. J. Julier and J. K. Uhlmann, "Unscented filtering and nonlinear estimation," *Proc. IEEE*, vol. 92, no. 3, pp. 401–422, Mar. 2004.

[4] I. Arasaratnam and S. Haykin, "Cubature Kalman filters," *IEEE Trans. Autom. Control*, vol. 54, no. 6, pp. 1254–1269, May 2009.

[5] B. Widrow, I. Kollar, and M.-C. Liu, "Statistical theory of quantization," *IEEE Trans. Instrum. Meas.*, vol. 45, no. 2, pp. 353–361, Apr. 1996.

[6] E. J. Msechu, S. I. Roumeliotis, A. Ribeiro, and G. B. Giannakis, "Decentralized quantized Kalman filtering with scalable communication cost," *IEEE Trans. Signal Process.*, vol. 56, no. 8, pp. 3727–3741, Aug. 2008.

[7] P. Carbone, J. Schoukens, I. Kollar, and A. Moschitta, "Accurate sine-wave amplitude measurements using nonlinearly quantized data," *IEEE Trans. Instrum. Meas.*, vol. 64, no. 12, pp. 3201–3208, Dec. 2015.

[8] X. Yang, R. Niu, E. Masazade, and P. K. Varshney, "Channel-aware tracking in multi-hop wireless sensor networks with quantized measurements," *IEEE Trans. Aerosp. Electron. Syst.*, vol. 49, no. 4, pp. 2353–2368, Oct. 2013.

[9] B. Chen, W.-A. Zhang, and L. Yu, "Distributed finite-horizon fusion Kalman filtering for bandwidth and energy constrained wireless sensor networks," *IEEE Trans. Signal Process.*, vol. 62, no. 4, pp. 797–812, Feb. 2014.

[10] B. G. Kermani, S. S. Schiffman, and H. T. Nagle, "A novel method for reducing the dimensionality in a sensor array," *IEEE Trans. Instrum. Meas.*, vol. 47, no. 3, pp. 728–741, Jun. 1998.

[11] B. Chen, W.-A. Zhang, L. Yu, G. Hu, and H. Song, "Distributed fusion estimation with communication bandwidth constraints," *IEEE Trans. Autom. Control*, vol. 60, no. 5, pp. 1398–1403, May 2015.

[12] E.-W. Bai, H. E. Baidoo-Williams, R. Mudumbai, and S. Dasgupta, "Robust tracking of piecewise linear trajectories with binary sensor networks," *Automatica*, vol. 61, pp. 134–145, Nov. 2015.

[13] B. F. L. Scala, M. R. Morelande, and C. O. Savage, "Robust target tracking with unreliable binary proximity sensors," in *Proc. IEEE Int. Conf. Acoust. Speed Signal Process. Proc.*, May 2006, p. 4.

[14] P. M. Djuric, M. Vemula, and M. F. Bugallo, "Target tracking by particle filtering in binary sensor networks," *IEEE Trans. Signal Process.*, vol. 56, no. 6, pp. 2229–2238, Jun. 2008.

[15] J. Teng, H. Snoussi, and C. Richard, "Decentralized variational filtering for target tracking in binary sensor networks," *IEEE Trans. Mobile Comput.*, vol. 9, no. 10, pp. 1465–1477, Oct. 2010.

[16] Q. L and L. M. Kaplan, "Target localization using proximity binary sensors," in *Proc. IEEE Aerosp. Conf.*, Mar. 2010, pp. 1–8.

[17] A. Shoari and A. Seyedi, "On localization of a non-cooperative target with non-coherent binary detectors," *IEEE Signal Process. Lett.*, vol. 21, no. 6, pp. 746–750, Jun. 2014.

[18] R. R. Tenney and N. R. Sandell, "Detection with distributed sensors," *IEEE Trans. Aerosp. Electron. Syst.*, vol. AES-17, no. 4, pp. 501–510, Jul. 1981.

[19] D. Ciuonzo and P. Salvo Rossi, "Distributed detection of a non-cooperative target via generalized locally-optimum approaches," *Inf. Fusion*, vol. 36, pp. 261–274, Jul. 2017.

[20] L. Y. Wang, Y.-W. Kim, and J. Sun, "Prediction of oxygen storage capacity and stored NO_x by HEGO sensors for improved LNT control strategies," in *Proc. Dyn. Syst. Control*, Jan. 2002, pp. 777–785.

[21] L. Y. Wang, J.-F. Zhang, and G. G. Yin, "System identification using binary sensors," *IEEE Trans. Autom. Control*, vol. 48, no. 11, pp. 1892–1907, Nov. 2003.

[22] R. Ivanov *et al.*, "Estimation of blood oxygen content using context-aware filtering," in *Proc. ACM/IEEE 7th Int. Conf. Cyber-Phys. Syst. (ICCPS)*, Apr. 2016, pp. 1–10.

[23] J. Sun and L. Li, "Online threshold tracking in cyber-physical-human systems based on binary observations," in *Proc. Amer. Control Conf. (ACC)*, Jul. 2020, pp. 1–12.

[24] A. Ribeiro, G. B. Giannakis, and S. I. Roumeliotis, "SOI-KF: Distributed Kalman filtering with low-cost communications using the sign of innovations," *IEEE Trans. Signal Process.*, vol. 54, no. 12, pp. 4782–4795, Dec. 2006.

[25] R. T. Sukhavasi and B. Hassibi, "The Kalman like particle filter: Optimal estimation with quantized innovations/measurements," in *Proc. 48h IEEE Conf. Decis. Control (CDC) Held Jointly With 28th Chin. Control Conf.*, Dec. 2009, pp. 4446–4451.

[26] G. Battistelli, L. Chisci, and S. Gherardini, "Moving horizon estimation for discrete-time linear systems with binary sensors: Algorithms and stability results," *Automatica*, vol. 85, pp. 374–385, Nov. 2017.

[27] Y. Zhang, B. Chen, and L. Yu, "Distributed fusion Kalman filtering under binary sensors," *Int. J. Robust Nonlinear Control*, vol. 30, no. 6, pp. 2570–2578, Apr. 2020.

[28] Y. Zhang, B. Chen, and L. Yu, "Fusion estimation under binary sensors," *Automatica*, vol. 115, May 2020, Art. no. 108861.

[29] B. Chen, G. Hu, D. W. C. Ho, and L. Yu, "Distributed estimation and control for discrete time-varying interconnected systems," *IEEE Trans. Autom. Control*, early access, Apr. 27, 2021, doi: 10.1109/TAC.2021.3075198.

[30] T. Wang, L. Xie, and C. E. de Souza, "Robust control of a class of uncertain nonlinear systems," *Syst. Control Lett.*, vol. 19, no. 2, pp. 139–149, 1992.

[31] W. Niehsen, "Information fusion based on fast covariance intersection filtering," in *Proc. Int. Conf. Inf. Fusion*, vol. 2. Annapolis, MD, USA, 2002, pp. 901–904.

[32] J. B. West, *Respiratory Physiology: The Essentials*. Baltimore, MD, USA: Lippincott Williams & Wilkins, 2012.

Zhongyao Hu received the B.E. degree in automation from Wuhan Polytechnic University, Wuhan, China, in 2019. He is currently pursuing the Ph.D. degree in control science and engineering with the Zhejiang University of Technology, Hangzhou, China.

His current research interests include nonlinear filter and networked fusion estimation systems.

Bo Chen (Member, IEEE) received the B.S. degree in information and computing science from the Jiangxi University of Science and Technology, Ganzhou, China, in 2008, and the Ph.D. degree in control theory and control engineering from the Zhejiang University of Technology, Hangzhou, China, in 2014.

He joined the Department of Automation, Zhejiang University of Technology, in 2018, where he is currently a Professor. He was a Research Fellow with the School of Electrical and Electronic Engineering, Nanyang Technological University, Singapore, from 2014 to 2015 and from 2017 to 2018. He was also a Post-Doctoral Research Fellow with the Department of Mathematics, City University of Hong Kong, Hong Kong, SAR, China, from 2015 to 2017. His current research interests include information fusion, distributed estimation and control, cyber-physical systems security, and networked fusion systems.

Dr. Chen was a recipient of the Outstanding Thesis Award of the Chinese Association of Automation (CAA) in 2015.

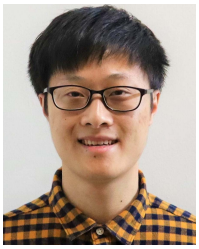

Yuchen Zhang (Graduate Student Member, IEEE) received the B.E. degree in automation from the Zhejiang University of Technology, Hangzhou, China, in 2017, where he is currently pursuing the Ph.D. degree in control science and engineering.

His current research interests include distributed estimation of interconnected systems, and fusion estimation of binary sensor systems.

Li Yu (Member, IEEE) received the B.S. degree in control theory from Nankai University, Tianjin, China, in 1982, and the M.S. and Ph.D. degrees from Zhejiang University, Hangzhou, China, in 1988 and 1999, respectively.

He is currently a Professor with the College of Information Engineering, Zhejiang University of Technology, Hangzhou. He has successively presided over 20 research projects. He has published five academic monographs, one textbook, and over 300 journal articles. He has also been authorized over 100 patents for invention and granted five scientific and technological awards. His current research interests include robust control, networked control systems, cyber-physical systems security, and information fusion.